Inorganic Chemistry Communications 150 (2023) 110457

Contents lists available at ScienceDirect

Inorganic Chemistry Communications

journal homepage: www.elsevier.com/locate/inoche

Short communication

Chemoradiation therapy of 4T1 cancer cells with methotrexate conjugated platinum nanoparticles under X-Ray irradiation

Kadir Yaray [a], Abdolvahed Norbakhsh [b], Hamid Rashidzadeh [b], Ali Mohammadi [b], Faezeh Mozafari [b], Mohammadreza Ghaffarlou [c], Navid Mousazadeh [b], Reza Ghaderzadeh [b], Yadollah Ghorbani [d], Leila Nasehi [e], Hossein Danafar [b,*], Yavuz Nuri Ertas [f,g,*]

[a] Department of Radiation Oncology, Faculty of Medicine, Erciyes University, Kayseri, Turkey
[b] Zanjan Pharmaceutical Biotechnology Research Center, Zanjan University of Medical Sciences, Zanjan, Iran
[c] Hacettepe University, Department of Chemistry, Beytepe, Ankara 06800, Turkey
[d] Department of Medical Radiation Engineering, Science and Research branch, Islamic Azad University, Tehran, Iran
[e] Department of Medical Laboratory, School of Paramedical Sciences, Zanjan University of Medical Sciences, Zanjan, Iran
[f] Department of Biomedical Engineering, Erciyes University, Kayseri 38039, Turkey
[g] ERNAM-Nanotechnology Research and Application Center, Erciyes University, Kayseri 38039, Turkey

ARTICLE INFO

Keywords:
Radiation therapy
Combination therapy
Platinum
Methotrexate
X-Ray

ABSTRACT

Bovine serum albumin (BSA) coated platinum (Pt) nanoparticles (Pt@BSA NPs) were synthesized, followed by the conjugation of an anticancer drug (MTX) with the aim of chemoradiation therapy. The physical and chemical properties of Pt@BSA-MTX were evaluated by DLS, FESEM, STEM, UV–Vis and XRD. A release study was performed in the presence and absence of the proteinase K enzyme. In terms of morphology, nanoparticles appeared to be monodispersed and spherical. The size of nanoparticles was 7.4 ± 1.4 nm. Release behavior of Pt@BSA-MTX depended significantly on enzyme presence which accelerated and promoted the release of MTX. The improved chemoradiation was demonstrated in vitro using MTT, colony formation and apoptosis assays on mouse breast carcinoma cells (4T1). It was concluded that the combination of a nanoradiosensitizer with a chemotherapeutic agent resulted in superior anticancer activity after X-ray exposure.

1. Introduction

Cancer is one of the most dangerous diseases, and its treatment is still challenging. There are many treatment approaches to cancer therapy, such as radiotherapy (RT), chemotherapy, hormonal therapy, immunotherapy and surgery [1–3]. Common clinical practice to cure and manage cancer is mostly focused on chemotherapy, radiation therapy and surgery [4]. Nevertheless, these treatments, when used individually, present many side effects and low therapeutic efficacy due to their nonspecific distribution [5]. Lately, combination therapies have received significant attention due to their potential to provide higher efficacy and reduce adverse effects. Furthermore, combination therapy is able to overcome drug resistance and reduce the treatment period due to its additive or synergistic effects.

Radiation therapy was discovered as one a cancer treatment more than a century ago [6]. Its mechanism involves damaging cancer cell DNA and genes that are responsible for cell growth and replication [7]. Radiation can cause DNA damage directly when it hits the DNA structure and indirectly through the induced generation of reactive oxygen species (ROS), which can induce oxidative stress and provoke damage to biomolecules and eventually cell death [8].

Radiosensitizers are agents that possess the capacity to substantially enhance the efficacy of radiotherapy on tumor cells through increasing tumor radiosensitivity [9]. They are able to reduce side effects because there are lower doses of radiation required [10]. The X-ray absorption coefficient (μ) describes the relationship between X-ray absorption energy (E), atomic number (Z) and densities (ρ), $\mu = \rho Z^4/AE^3$,where A is atomic mass of elements [8,11]. As a result, high Z-elements such as platinum (Pt), gold, bismuth, and others have better X-ray absorption and the ability to localize ionizing radiation doses at tumor tissue [12]. Radiosensitizers can absorb X-ray radiation and then scatter photo/Auger/Compton and other secondary electrons, so they can cause DNA damage directly and are also able to react with water and increase ROS production, leading to enhanced tumor cell radiosensitivity [13].

* Corresponding authors at: ERNAM-Nanotechnology Research and Application Center, Erciyes University, Kayseri 38039, Turkey (Y.N. Ertas).
E-mail addresses: danafar@zums.ac.ir (H. Danafar), yavuzertas@erciyes.edu.tr (Y.N. Ertas).

https://doi.org/10.1016/j.inoche.2023.110457
Received 3 August 2022; Received in revised form 30 December 2022; Accepted 25 January 2023
Available online 1 February 2023

Nanoparticles (NPs) can accumulate within tumors via the enhanced permeability and retention (EPR) effect and consequently increase radiation doses within tumor cells [14].

Studies have shown that Pt NPs can be used as a radiosensitizer due to the high atomic number (Z = 78) of Pt [15]. Yang *et al.* presented enhanced radiotherapy using Au-Pt NPs as a radiosensitizer, substantially inhibiting tumor growth [16]. Pt nanoflowers have also been shown to enhance gamma ray-induced killing of HeLa cells with a sensitizing enhancement ratio (SER) of 23% [17].

NPs can be used for the drug delivery of chemotherapy drugs due to their exclusive characteristics [18,19]. Therefore, the high Z based nanoparticles can be used not only as a radiosensitizer but also as drug carriers to the tumor site. Drug delivery with NPs can overcome multidrug resistance due to their ability to bypass efflux pumps. NPs can transport chemotherapeutic drugs into tumor cells through endocytosis and release the payload at the perinuclear site, which is distant from efflux pumps. Through the EPR effect and passive targeting, NPs can increase the concentration of drugs within the tumor site [20].

Methotrexate (MTX), an analog of folic acid, is a non-selective inhibitor of dihydrofolate reductase (DHFR) [21]. However, there is evidence that MTX itself can act as a particular tumor-targeting ligand by binding to folate receptors that are overexpressed in the vast majority of solid tumors and cancer cell lines [22]. MTX is still a viable ligand for tumor-specific drug delivery [23]. In order to be used as carriers of one-carbon groups in the synthesis of purine nucleotides and thymidylate, and therefore DNA synthesis, dihydrofolates must be converted to tetrahydrofolates by DHFR. Anti-folates, as inhibitors of DHFR, have several therapeutic applications, including as anti-infective, anti-neoplastic, and anti-inflammatory drugs. These medications affect more actively proliferating tissues such as cancer cells, fetal cells, bone marrow, and the buccal and intestinal mucosa. In this line, Koda *et al.* applied pemetrexed, a multitargeted antifolate, in combination with cisplatin for the treatment of malignant pleural mesothelioma [24]. MTX is a folate antimetabolite that inhibits DNA synthesis, repair, and replication, and it is used in the treatment of various types of cancer. In the clinics, MTX is commonly utilized as an immunosuppressive, anti-inflammatory, and anticancer agent [25]. MTX is also used for the treatment of alopecia areata in combination with oral corticosteroids and the immune system in the skin (diphencyprone) [26,27].

Because of its severe side effects in high doses, researchers attempted to use novel drug delivery vehicles in order to reduce side effects and enhance therapeutic efficacy. Combination therapies are another way to lower the dose needed. When radiation therapy and chemotherapy are used together, the outcome of the treatment is much better.

Albumin is a biological molecule that is one of the most abundant plasma proteins, and due to its unique features, it can be used as a carrier for medicines [28]. Its most important characteristics include minimal toxicity, easy preparation, biodegradability, multiple ligand binding sites, a long half-life, and stability in circulation that can be used in order to coat and stabilize NPs such as Pt in biological medium [29–31].

In this study, we report Pt NPs coated with bovine serum albumin (BSA) and loaded with the MTX drug, which functions as both a radiosensitizer and drug carrier to improve therapeutic efficiency. Combination therapy of chemotherapy along with radiation therapy provided enhanced tumor treatment, which was validated using mouse breast carcinoma cells (4T1).

2. Materials and methods

2.1. Materials

All material and solutions were purchased from Sigma Aldrich and Merck Co.

2.2. Synthesis of Pt@BSA NPs

Bovine serum albumin-coated Pt (Pt@BSA) NPs were synthesized as follows: First, 5 mL of an aqueous solution of BSA (8 mg/mL) was mixed with 5 mL of H_2PtCl_6 (16 mM), and then 0.5 mL of NaOH (1.5 M) was added to the reaction medium. The solution was allowed to react overnight at 80 °C. After 24 h, as-synthesized Pt@BSA was purified by dialysis against deionized water for 24 h [32].

2.3. Preparation of MTX conjugated Pt@BSA (Pt@BSA-MTX)

For the preparation of Pt@BSA-MTX, 100 mg of MTX, 183 mg of 1-ethyl-3-(3-dimethylaminopropyl) carbodiimide (EDC), and 21.85 mg of N-hydroxysuccinimide (NHS) were first mixed in 20 mL of deionized water. After 15 min, 400 mg of Pt@BSA was added to the mixture. Solution was stirred in dark and room temperature for 24 h. To remove excess material, final product was dialyzed against deionized water for 48 h.

2.4. Characterization

Field emission scanning electron microscopy (FESEM) and scanning transmission electron microscope (STEM) (ZEISS GeminiSEM) were used to characterize the size and morphology of synthesized NPs. The hydrodynamic size distributions were evaluated by a dynamic light scattering (DLS) device (Malvern Instruments, Worcestershire, UK, model Nano ZS). UV–Vis absorption spectra were acquired via a UV–Vis spectrophotometer (T80). To reveal the crystal structures, a powder X-ray diffractometer system (PANalytical X'Pert Powder Diffractometer) was used.

2.5. Drug loading

To determine the content of conjugated MTX, 3 mg of Pt@BSA-MTX NPs and 3 mg of proteinase K enzyme were added to 2 mL of phosphate-buffered saline (PBS) (pH = 7) and incubated for 48 h at 37 °C. Then, the Eppendorf cells were centrifuged, and the absorbance of the supernatant was measured by UV–Vis spectrophotometry at a wavelength of 304 nm. Finally, the amount of conjugated MTX was calculated using the calibration curve.

2.6. Drug release study

The release study of MTX was determined by a dialysis method. Drug release was performed in the presence and absence of the proteinase K enzyme. Considering the first condition, 2 mg of Pt@BSA-MTX and 1 mg of proteinase K enzyme were dispersed in 1 mL of PBS (pH = 7.4 or 4.8) and then poured into a dialysis bag (12 kDa). Next, the dialysis bag was submerged in a container with 20 mL of PBS that was shaken at 37 °C and 100 rpm. 2 mL of dialysate medium was taken out of the solution at different programmed time intervals and replaced with PBS. Thereupon, the absorbance of the isolated solution was measured at 304 nm by a UV–Vis spectrophotometer. The same protocol was performed in the absence of the proteinase K enzyme.

2.7. In vitro treatment efficacy

The viability of mouse breast carcinoma cells (4T1) treated with Pt@BSA-MTX NPs under and without X-ray irradiation was examined by an MTT assay. First, the cells were seeded into 96-well microplates at a density of 5000 cells per well and then cultured in a humidified incubator in RPMI medium supplemented with 10% fetal bovine serum at a temperature of 37 °C and 5% CO_2. The cells were incubated for 24 h. Then, the medium of each well was substituted for various concentrations of Pt@BSA-MTX NPs. After 5 h of treatment, the medium containing the sample extract and the wells was washed with PBS and then

filled with fresh RPMI. After the exposure of cells to X-rays (4 Gy, 6 MV), the cell viability of each well was determined via MTT assays.

2.8. Colony formation assay

The colony formation assay revealed the cell survival by measuring single cell's ability to grow and form a colony. Thus, to exploit the potential of the radiosensitizing capacity of developed NPs in the presence of X-ray irradiation, a clonogenic assay was performed according to the previously reported method [9].

2.9. Apoptosis assays

To assess apoptosis, 4T1 cells were seeded into a 12-well plate and cultured for 24 h. Then, the medium of each well was substituted for various samples. After 5 h of incubation, the medium containing the sample was extracted, and the wells were washed with PBS and filled with fresh RPMI. The cells were irradiated with X-ray radiation at a dose of 4 Gy, followed by incubation. Later, the treated cells were taken out and fully washed with PBS, then added to 100 μL Annexin V binding buffer, stained with Annexin V-FITC and propidium iodide. In the final step, stained cells were determined by flow cytometry, and data analysis was carried out by FLOWJO software (Tree Star, Ashland, OR).

3. Results and discussions

3.1. Characterization

The characterization of any developed metal nanoparticle-based radiosensitizer in terms of elemental composition, crystal structure, morphology, and size mostly involves various types of analytical tools. Even in some cases, more than one technique is required to evaluate the physical properties of designed nanoparticles. SEM, as a powerful technique, was used to investigate the size, homogeneity, and morphology of as-synthetized nanoparticles, which is depicted in Fig. 1a. In terms of morphology, nanoparticles appeared to be homogenous and monodispersed. STEM image (Fig. 1b) further shows that the shape and size of the nanoparticles were spherical and 7.4 ± 1.4 nm in size. Similar to SEM results, STEM images also show monodispersed and spherical nanoparticles, confirming the successful preparation of Pt@BSA-MTX NPs. The size of the nanoparticles was less than 8 nm, and mostly no indication of aggregation was evident, which validates their stability. UV–Vis spectrophotometry was performed as the preliminary characterization technique to confirm the successful formation of the designed nanoradiosensitizers. Also, this technique was applied to study possible interactions between different compounds in the structure of a prepared metal nanoparticle-based radiosensitizer. Fig. 1c shows the UV–Vis spectra of free MTX, Pt@BSA, and Pt@BSA-MTX. It is obvious that the main absorbance peaks of MTX drugs are assigned at around 373 nm and 303 nm. Typically, an absorption peak at around 275 nm is assigned for BSA due to the presence of tryptophan and tyrosine groups in its structure. Previously, it was well documented that H_2PtCl_6 solution, due to its d–d transitions, showed bands at approximately 320 and 380 nm [33]. As shown in Fig. 1c, no peak was detected for Pt@BSA nanoparticles between 300 and 400 nm, and the absorption peaks of H_2PtCl_6 were completely disappeared due to the reduction reaction, leaving only an absorption peak at around 271 nm, which can be attributed to the presence of BSA macromolecules [34]. These results were also observed in UV–Vis spectrum of Pt@BSA-MTX nanoparticles, in which Pt nanoparticles had no peaks in the range of 300–400 nm and

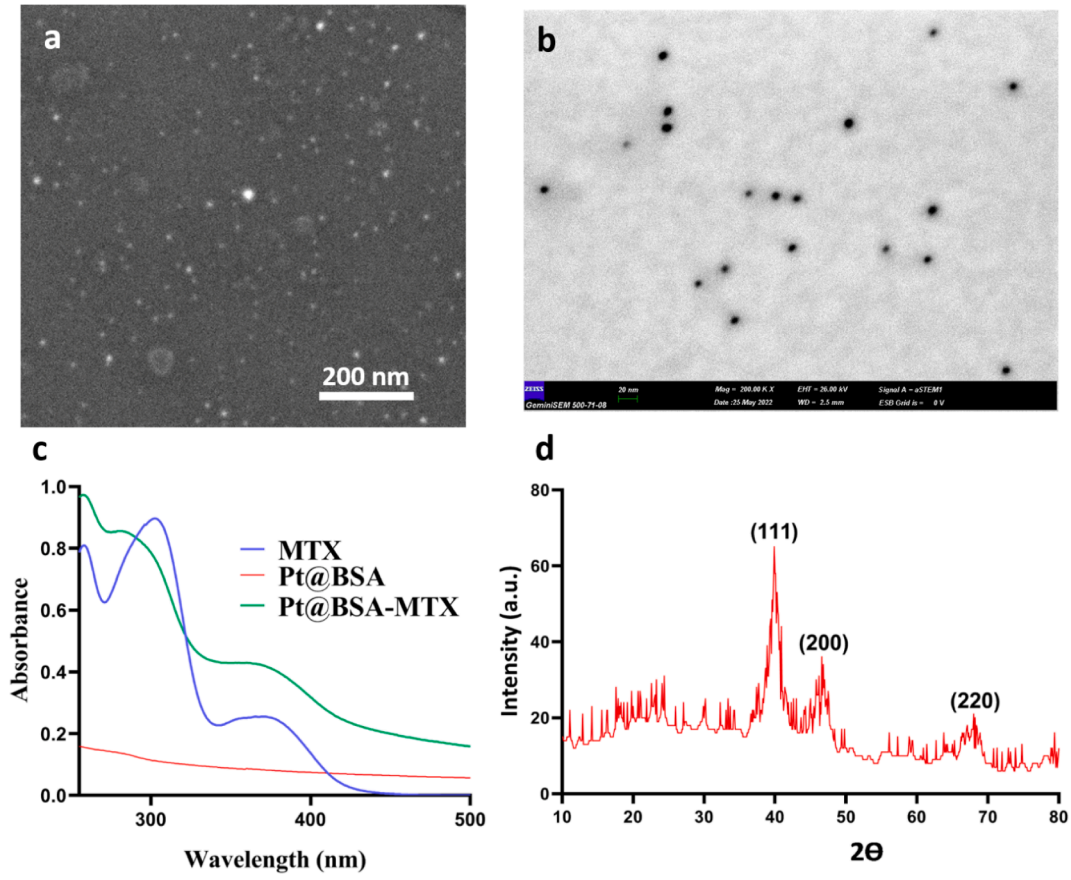

Fig. 1. Characterization techniques regarding to the developed nanoparticles. (a) Fe-SEM; (b) STEM image of Pt@BSA-MTX nanoparticles; (c) UV–Vis spectra of MTX, Pt@BSA, and Pt@BSA-MTX; and (d) XRD pattern of developed metallic nanoparticles.

only characteristic peaks of MTX along with BSA protein were observed with slight peak shifting. It can be implied that Pt@BSA-MTX nanoformulations were successfully prepared. These results are consistent with previous findings in the literature [35,36]. Besides, UV–Vis analysis disclosed the amount of MTX entrapment in the Pt@BSA was approximately 6.3%. X-ray diffraction (XRD) analysis is a non-destructive technique, and owing to its speed and simplicity, it has gained much popularity in the identification of a wide variety of designed metallic nanoparticles [37]. In particular, XRD analysis is performed to assess elemental composition, crystallinity, and phase purity. Additionally, this technique could provide information regarding the crystalline grain size and lattice parameters. Fig. 1d illustrates the XRD spectrum of Pt@BSA. There were several index planes for different values of 2θ as illustrated by the XRD pattern in Fig. 1d. This finding showed that Pt@BSA nanoradiosensitizers possessed face-centered-cubic (FCC) structure according to JCPDS file No. 04-0802 [38]. Four characteristic reflections were observed in the XRD pattern for Pt@BSA NPs, which correspond to the (1 1 1), (2 0 0), and (2 2 0) crystal lattice planes and are consistent with the FCC structure. This result further validates that Pt@BSA nanoradiosensitizers were properly synthesized and can be employed for in vitro analysis.

3.2. Hydrodynamic size and zeta potential

Zeta potential is influential in the primary adsorption and interaction of nanomaterials with extracellular biological macromolecules, including those on the cell membrane [39]. Following initial interaction, endocytosis is the next process of immense importance, and the size of the nanoparticles plays a key role in the uptake rate. Therefore, hydrodynamic size and zeta potential were demonstrated for both Pt@BSA-MTX and Pt@BSA. The hydrodynamic sizes of Pt@BSA and Pt@BSA-MTX are on average 49 nm and 28 nm (Fig. 2a), respectively, which are desirable for efficient drug delivery due to their being less than 100 nm [40]. Polydispersity indexes (PdI) are also determined as 0.312 and 0.347 for Pt@BSA and Pt@BSA-MTX, respectively. The average particle size of Pt@BSA-MTX is consistent with SEM results but higher than that observed in a TEM image, which is probably due to minor swelling of nanoparticles in aqueous media.

Hydrodynamic size monitoring was also further used for the determination of colloidal stability for up to two months (Fig. 2b). Results showed that the hydrodynamic size of NPs reached 64 nm, yet it still remained desirable for in vivo anticancer performance such as tissue penetration and tumor inhibition [41]. Zeta potential is defined as the surface charge of nanoparticles, which is necessary for stability and preventing aggregation of nanoparticles in biological media, profoundly affecting in vivo applications. The zeta potentials measured for Pt@BSA and Pt@BSA-MTX were approximately −22 mV and −25 mV, respectively (Fig. 2c). Data shows that the zeta potentials of prepared nanoparticles are favorable, as higher charge values manifest enhanced stability [42]. Although there was a significant increase in particle size, the zeta potential alternation was negligible after MTX conjugation. Evidently, owing to the large negative surface charge of as-synthetized nanoparticles, they significantly repel each other in a suspension and have the least interaction with blood components (noting their negative charge), which makes them favorable for entering blood flow. Negative surface charge is superior to positive charge for nanoparticles, which provides them with prolonged blood circulation time and improved stability. In summary, the size and zeta potential of Pt@BSA-MTX NPs nanoparticles were found to be advantageous for cancer treatment and stable for medical applications.

3.3. In vitro drug release study

MTX release from nanoparticles was investigated with and without proteinase K, an enzyme that breaks the amide bond between conjugated MTX and albumin. The release behavior of MTX under lysosomal conditions (intracellular) represents a high enzyme impact on drug release from nanoparticles (Fig. 2d). In the absence of enzyme, the cumulative amount of drug rose steadily to approximately 17% of the total drug amount within 24 h, whereas in the presence of enzyme, the amount of drug released increased sharply and reached as high as 71% within the same period of time. Following this sharp increase, the amount of drug released from nanocarriers increased slightly to 75% after 48 h and then plateaued. Similarly, without enzymes, drug release remained fairly steady and finally reached 19%. At 24 h, compared to the absence of enzyme, cumulative drug release in the presence of enzyme drastically. Thus, the release behavior of Pt@BSA-MTX depends significantly on the presence of an enzyme, which accelerates and promotes MTX release [43]. Previous studies demonstrated that the bond between MTX and modified nanoparticles can be hydrolyzed in an

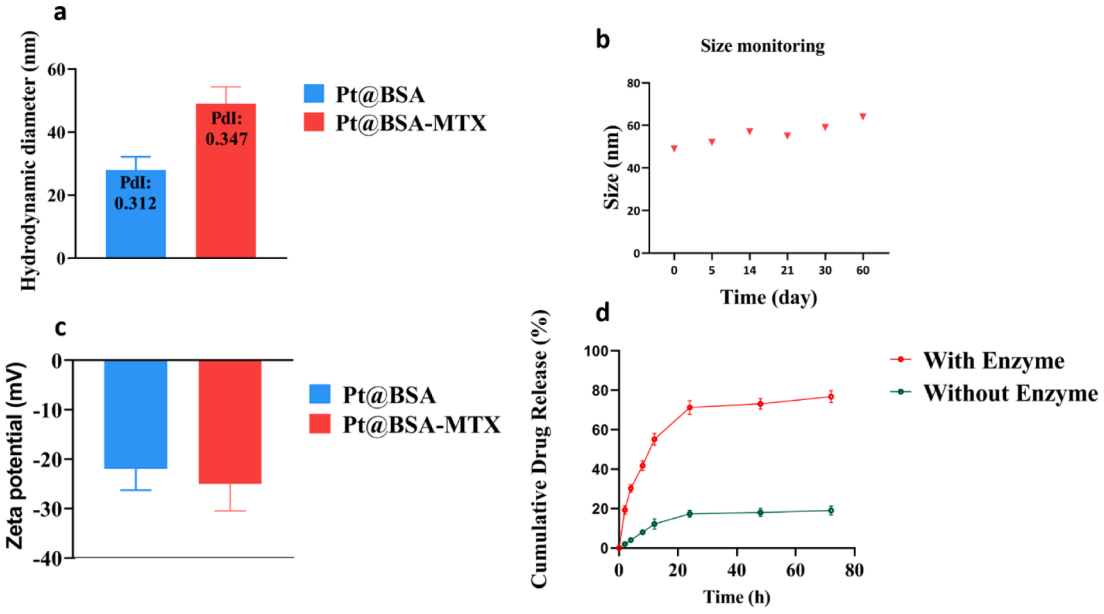

Fig. 2. (a) Mean hydrodynamic particle size; (b) Size monitoring of Pt@BSA-MTX NPs for two months; (c) zeta potential of Pt@BSA-MTX nanoparticles and (d) Drug release profile of developed metallic nanoparticles.

intracellular enzymatic condition, which causes the release of MTX and cell cycle arrest [44,45]. Thus, the amide bond can be utilized for accelerating drug release inside cancer cells. Under physiological conditions (pH = 7.4, mimics blood circulation), drug release from nanoparticles was significantly higher in enzyme presence compared with its absence, implying the existence of the amido bond, which assists with the delivery of drug to the targeted cell. This could be another confirmation of the successful synthesis of Pt@BSA-MTX in our study. In summary, this release behavior can alleviate chemotherapy-associated side effects and improve treatment efficacy, noting that drug release depends greatly on enzyme presence inside the lysosome, the next destination of nanoparticles after endocytosis.

3.4. *In vitro radiotherapy of Pt@BSA-MTX nanoparticles*

RT is always a balance between alleviating damage to the healthy tissues and destroying the tumor tissues. However, minimizing the adverse effects of RT remains an ongoing challenge in cancer radio oncology. To this end, vast efforts have been put forth to diminish the associated side effects of RT as a result of the non-selective nature of radiation. In recent years, metallic radiosensitizers as multifunctional nanoplatforms have emerged as a very promising strategy in cancer radiotherapy, owing to their effectiveness in therapeutic index enhancement and selective tumor responses to RT. The latest advances in the development of metal nanoparticle-based radiosensitizers stand out as a novel cancer treatment modality with high success and effectiveness while being non-invasive and affordable to patients. Furthermore, the in vitro anticancer effect of developed Pt@BSA-MTX nanoparticles upon X-ray radiation was evaluated in addition to the in vitro findings of X-ray radiotherapy, such as apoptosis and colony formation assays. Fig. 3 depicts the in vitro radiotherapy or radiosensitization effects of MTX, Pt@BSA, and Pt@BSA-MTX in the presence and absence of X-ray irradiation. Exposure of 4T1 cells to X-ray radiation at a dose of 4 Gy resulted in reduced cell viability (82%). This points to the pivotal role of X-ray radiation in cancer radiotherapy, but this method of cancer treatment alone is not efficient enough to cure cancer unless higher doses of radiation are applied. However, a radiation dose increase can also pose a greater risk to healthy tissue nearby; thus, the importance of X-ray radiation cannot be emphasized enough. It is interesting to note that there is a statistically significant difference in cell viability rate between treated groups and controls, except for the cells treated with Pt@BSA (60 μg/mL). Combined treatment with X-ray radiation resulted in a significant reduction of cell viability compared to monotherapy for all experimental groups. These results underline the superior performance and advantage of combined therapy over monotherapy. The cell survival rates for Pt@BSA and Pt@BSA-MTX nanoparticles at a concentration of 60 μg/mL were 95% and 80%, respectively. By increasing the concentration of nanoparticles from 60 to 300 μg/mL, the corresponding cell viability was reduced to 87% and 68%, respectively. This indicates that the developed nanoparticles kill cancer cells in a dose-dependent manner. Similar results were also observed for the Pt@BSA and Pt@BSA-MTX nanoparticles in the presence of X-ray irradiation. At a concentration of 60 μg/mL, the cell viability was reduced to 63% and 47% after X-ray exposure for Pt@BSA and Pt@BSA-MTX, respectively. Furthermore, by increasing the concentration of treatment groups from 60 to 300 μg/mL, the cell viability dropped from 58% to 39%. In addition to the dose dependency effects, these findings highlight the potential ability of prepared nanoparticles to sensitize cancer cells to radiation therapy by lowering cancer cell survival rates. We speculate the effect of nanoparticles arises from the capability of Pt nanoparticles to enhance ROS production upon X-ray irradiation, which is in agreement with previous studies [15,16]. Moreover, the addition of BSA to Pt nanoparticles improved their biocompatibility and stability, while conjugated MTX contributed to the inhibition of cell growth, which is in line with previous findings [15,46]. Jiang *et al.* prepared the multifunctional nanoplatform $MnSiO_3$-Pt@BSA-Ce6 (MPBC) for enhanced chemodynamic and sonodynamic cancer therapy and diagnosis. The results disclosed that the designed nanoplatform, due to the presence of Pt and BSA, had the ability to kill cancer cells effectively and safely, augmenting the therapeutic efficacy through combined therapy. Overall, in vitro radiotherapy results prove that cells are more sensitive to radiation in the presence of designed nanoparticles, specifying the usefulness of nanoradiosensitizers in radiation-induced cancer therapy.

3.5. *Colony formation assay*

The colony formation assay is the commonly used method to assess the potential radiosensitizing capability of nanoparticles, in which survival cell fractions are determined after exposure to ionizing radiation in the presence of prepared nanoradiosensitizers. Accordingly, to elucidate the effectiveness of the designed nanoparticles, the colony formation assay was performed. Fig. 4 illustrates the radiosensitization capability of X-ray, MTX, Pt@BSA-MTX and using Pt@BSA-MTX + X-ray using in vitro clonogenic assay. Results revealed that cell sensitization occurred in 4T1 cells in which suppression of cell growth were observed in cells treated with different treatment options including X-ray, MTX, Pt@BSA-MTX and using Pt@BSA-MTX + X-ray. In other words, while all of the modalities mentioned above can statistically reduce the colony formation numbers when compared to controls, their ability to induce cell death varies greatly. The survival fraction of 4T1 cells exposed to X-ray alone or MTX decreased to ~0.9% and ~0.73%, respectively, while that in groups treated with Pt@BSA-MTX noticeably decreased to ~0.64%, meaning that Pt@BSA-MTX nanoparticles display a superior cell

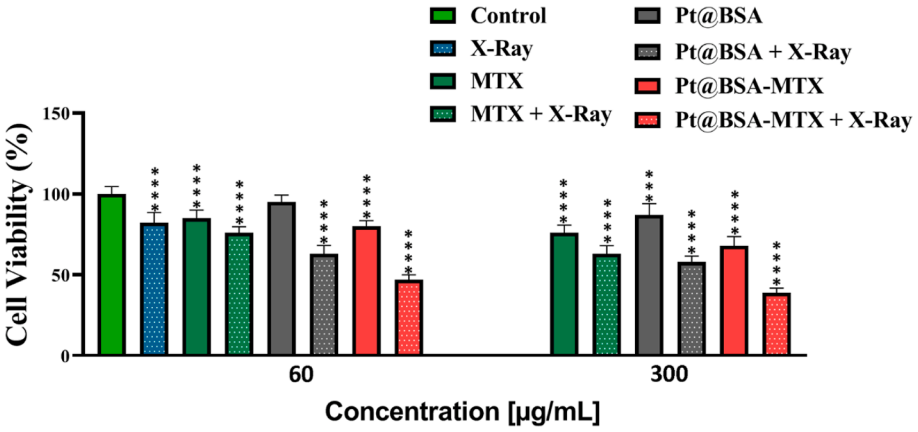

Fig. 3. *In vitro* radiosensitization capacity of developed Pt@BSA-MTX nanoplatforms by MTT assay.

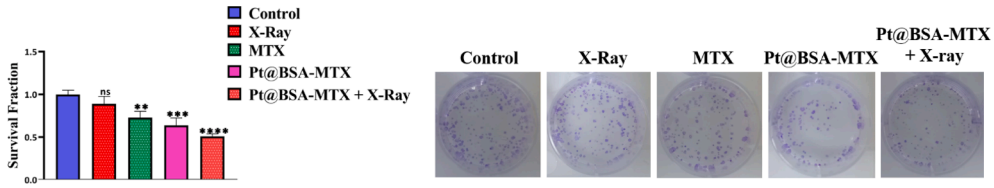

Fig. 4. *In vitro* radiosensitization capacity of developed Pt@BSA-MTX nanoplatforms by colony formation assay.

antigrowth effect compared to MTX or X-ray alone. The most notable result from the data is that combined treatment with Pt@BSA-MTX nanoparticles and an X-ray modality resulted in a great radiosensitization effect in which the survival fraction dropped to ~0.51%. In summary, the potential capability of these modalities in reduction of the colony formation numbers are as follows: X-ray < MTX < Pt@BSA-MTX < Pt@BSA-MTX + X-ray. Of note, this result lends support to previous findings in the literature and concurs well with them. Yang *et al.* developed PEGylated Pt nanoflowers for enhanced cancer radiotherapy, where the cell fraction treated with Pt nanoflowers upon radiation dramatically decreased, indicating the radiosensitizing capability of Pt nanoflowers [17]. This outcome has further strengthened our conviction for the usefulness of the designed Pt@BSA-MTX as a promising nano-radiosensitizer in cancer radiotherapy with positive therapeutic efficacy.

3.6. Apoptosis assay in 4T1 cell line

Apoptosis rate was assessed after cell treatment with MTX, X-ray, Pt@BSA-MTX and Pt@BSA-MTX + X-ray. Results were compared statistically with the control group, indicating a significant change in apoptosis level after different treatments. The rate of cell apoptosis increased more significantly (by 42 %) when cells were treated with Pt@BSA-MTX and irradiation simultaneously, compared to other treatments (Fig. 5). Also, apoptotic cell death is clearly higher in the group treated with Pt@BSA-MTX in comparison with the group of cells treated with the free form of MTX. The apoptosis rate is considerably higher in the Pt@BSA-MTX group when accompanied by radiotherapy in comparison to the Pt@BSA-MTX group, which is probably due to the radiosensitizing feature of Pt. Pt radiosensitizing capability was previously demonstrated in vitro on the cancerous A549 lung cell line by inducing apoptosis, but no effect on the healthy cell line, MRC-5 embryonic lung fibroblasts, was observed. It could be concluded that treatment of cells with Pt-based nanomaterials can amplify the radiation's impact on cancerous cells [47]. It should be noted that apoptosis rate is significantly higher in all cell groups, especially Pt@BSA-MTX and Pt@BSA-MTX + X-ray group. Apoptosis induced by different treatments are as follows: Pt@BSA-MTX + X-ray > Pt@BSA-MTX > MTX > X-ray > Control. There was a drop in viable cell count trend in the graph depicting apoptosis rate after irradiation and exposure to therapeutic agents. Thus, it could be concluded that the combination of a nanoradiosensitizer with a chemotherapeutic agent in the case of X-ray exposure results in a superior apoptotic rate and is thus more efficient in cancer treatment.

4. Conclusion

In this work, we developed MTX-conjugated Pt@BSA NPs (Pt@BSA-MTX) for use in chemotherapy therapy. MTX was conjugated with an enzymatically cleavable amide bond. Pt@BSA-MTX was utilized as both a radiosensitizer and a MTX carrier. A drug release study revealed an enzyme-dependent release characteristic. Mouse breast carcinoma cells (4T1) were used to evaluate the tumor-killing efficacy of the treatment groups. Both cell viability and clonogenic assays revealed that the superior anticancer potential of Pt nanoparticles was observed when the anticancer drug and X-ray were applied together, confirming the benefit

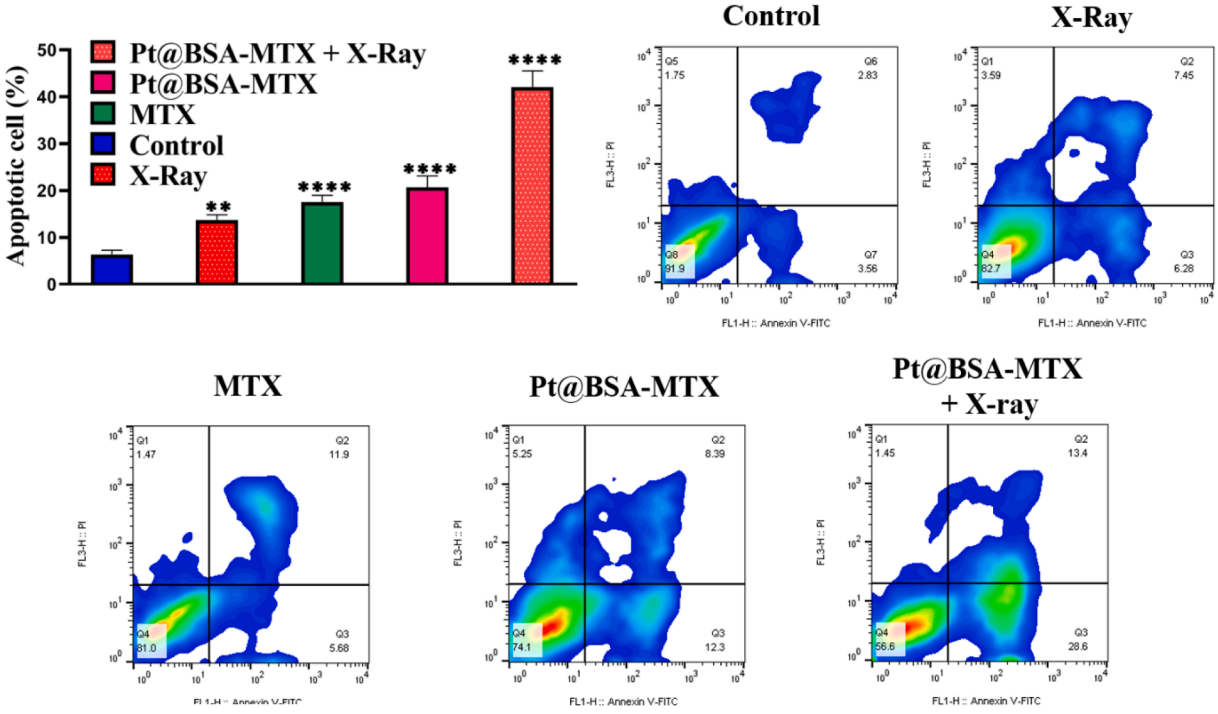

Fig. 5. Apoptosis assay result of cells treated with different samples.

of chemotherapy and radiation therapy when applied in a synergistic manner.

CRediT authorship contribution statement

Kadir Yaray: Data curation, Methodology, Validation. **Abdolvahed Norbakhsh:** Data curation, Investigation, Methodology. **Hamid Rashidzadeh:** Data curation, Investigation, Writing - original draft. **Ali Mohammadi:** Investigation, Methodology. **Faezeh Mozafari:** Formal analysis, Investigation, Writing - original draft. **Mohammadreza Ghaffarlou:** Data curation, Formal analysis, Software. **Navid Mousazadeh:** Formal analysis, Investigation, Methodology. **Reza Ghaderzadeh:** Software, Writing - original draft. **Yadollah Ghorbani:** Investigation, Methodology. **Leila Nasehi:** Formal analysis, Methodology, Resources. **Hossein Danafar:** Funding acquisition, Project administration, Supervision, Writing - review & editing. **Yavuz Nuri Ertas:** Funding acquisition, Project administration, Supervision, Data curation, Resources, Software, Writing - original draft, Writing - review & editing.

Declaration of Competing Interest

The authors declare that they have no known competing financial interests or personal relationships that could have appeared to influence the work reported in this paper.

Data availability

Data will be made available on request.

Acknowledgments

This work was supported by the Deputy of Research of Zanjan University of Medical Sciences (grant no. A-12-430-46). Y. N. Ertas acknowledges funding support from the 2232 International Fellowship for Outstanding Researchers Program of TÜBİTAK (Project No: 118C346).

Data availability statement

The raw/processed data required to reproduce these findings cannot be shared at the moment, as the data also forms part of an ongoing study.

References

[1] M. Ashrafizadeh, A. Zarrabi, H. Karimi-Maleh, A. Taheriazam, S. Mirzaei, M. Hashemi, et al. (Nano) platforms in bladder cancer therapy: Challenges and opportunities, Bioeng. Translat. Med., e10353.
[2] W. Wei, N. Zarghami, M. Abasi, Y.N. Ertas, Y. Pilehvar, Implantable magnetic nanofibers with ON–OFF switchable release of curcumin for possible local hyperthermic chemotherapy of melanoma, J. Biomed. Mater. Res. A 110 (4) (2022) 851–860.
[3] M. Salehiabar, M. Ghaffarlou, A. Mohammadi, N. Mousazadeh, H. Rahimi, F. Abhari, et al., Targeted CuFe2O4 hybrid nanoradiosensitizers for synchronous chemoradiotherapy, J. Control. Release 353 (2023) 850–863.
[4] Y. Chen, G. Song, Z. Dong, X. Yi, Y. Chao, C. Liang, et al., Drug-loaded mesoporous tantalum oxide nanoparticles for enhanced synergetic chemoradiotherapy with reduced systemic toxicity, Small 13 (8) (2017) 1602869.
[5] N. Jan, A. Madni, S. Khan, H. Shah, F. Akram, A. Khan, et al., Biomimetic cell membrane-coated poly (lactic-co-glycolic acid) nanoparticles for biomedical applications, Bioeng. Transl. Med. (2022) e10441.
[6] S. Gianfaldoni, R. Gianfaldoni, U. Wollina, J. Lotti, G. Tchernev, T. Lotti, An overview on radiotherapy: from its history to its current applications in dermatology, Open Access Macedonian J. Med. Sci. 5 (4) (2017) 521.
[7] H. Nosrati, M. Ghaffarlou, M. Salehiabar, N. Mousazadeh, F. Abhari, M. Barsbay, et al., Magnetite and bismuth sulfide Janus heterostructures as radiosensitizers for in vivo enhanced radiotherapy in breast cancer, Biomater. Adv. 140 (2022), 213090.
[8] L. Gong, Y. Zhang, C. Liu, M. Zhang, S. Han, Application of radiosensitizers in cancer radiotherapy, Int. J. Nanomed. 16 (2021) 1083.
[9] H. Nosrati, F. Seidi, A. Hosseinmirzaei, N. Mousazadeh, A. Mohammadi, M. Ghaffarlou, et al., Prodrug polymeric nanoconjugates encapsulating gold nanoparticles for enhanced X-Ray radiation therapy in breast cancer, Adv. Healthc. Mater. 11 (3) (2022) 2102321.
[10] F. Abhari, J. Charmi, H. Rezaeejam, Z. Karimimoghaddam, H. Nosrati, H. Danafar, et al., Folic acid modified bismuth sulfide and gold heterodimers for enhancing radiosensitization of mice tumors to X-ray radiation, ACS Sustain. Chem. Eng. 8 (13) (2020) 5260–5269.
[11] M. Hernández-Rivera, I. Kumar, S.Y. Cho, B.Y. Cheong, M.X. Pulikkathara, S. E. Moghaddam, et al., High-performance hybrid bismuth–carbon nanotube based contrast agent for X-ray CT imaging, ACS Appl. Mater. Interfaces 9 (7) (2017) 5709–5716.
[12] H. Wang, X. Mu, H. He, X.-D. Zhang, Cancer radiosensitizers, Trends Pharmacol. Sci. 39 (1) (2018) 24–48.
[13] A.G. Denkova, H. Liu, Y. Men, R. Eelkema, Enhanced cancer therapy by combining radiation and chemical effects mediated by nanocarriers, Adv. Therap. 3 (3) (2020) 1900177.
[14] Y. Yao, Y. Zhou, L. Liu, Y. Xu, Q. Chen, Y. Wang, et al., Nanoparticle-based drug delivery in cancer therapy and its role in overcoming drug resistance, Front. Mol. Biosci. (2020) 193.
[15] Y. Zhang, D. Zheng, S. Talaei, M. Abasi, Albumin stabilized Pt nanoparticles as radiosensitizer for sensitization of breast cancer cells under X-ray radiation therapy, Inorg. Chem. Commun. 140 (2022), 109423.
[16] S. Yang, G. Han, Q. Chen, L. Yu, P. Wang, Q. Zhang, et al., Au-Pt nanoparticle formulation as a radiosensitizer for radiotherapy with dual effects, Int. J. Nanomed. 16 (2021) 239.
[17] X. Yang, D. Salado-Leza, E. Porcel, C.R. González-Vargas, F. Savina, D. Dragoe, et al., A facile one-pot synthesis of versatile PEGylated platinum nanoflowers and their application in radiation therapy, Int. J. Mol. Sci. 21 (5) (2020) 1619.
[18] H. Nosrati, M. Salehiabar, F. Mozafari, J. Charmi, N. Erdoğan, M. Ghaffarlou, et al., Preparation and evaluation of bismuth sulfide and magnetite-based theranostic nanohybrid as drug carrier and dual MRI/CT contrast agent, Appl. Organomet. Chem. 36 (11) (2022) e6861.
[19] M. Hashemi, F. Ghadyani, S. Hasani, Y. Olyaee, B. Raei, M. Khodadadi, et al., Nanoliposomes for doxorubicin delivery: Reversing drug resistance, stimuli-responsive carriers and clinical translation, J. Drug Delivery Sci. Technol. 104112 (2022).
[20] Y.N. Ertas, K. Abedi Dorcheh, A. Akbari, E. Jabbari, Nanoparticles for targeted drug delivery to cancer stem cells: a review of recent advances, Nanomaterials 11 (7) (2021) 1755.
[21] Y. Lin, Y. Yang, K. Yuan, S. Yang, S. Zhang, H. Li, et al., Multi-omics analysis based on 3D-bioprinted models innovates therapeutic target discovery of osteosarcoma, Bioact. Mater. 18 (2022) 459–470.
[22] J.M. Rosenholm, E. Peuhu, L.T. Bate-Eya, J.E. Eriksson, C. Sahlgren, M. Lindén, Cancer-cell-specific induction of apoptosis using mesoporous silica nanoparticles as drug-delivery vectors, Small 6 (11) (2010) 1234–1241.
[23] Y. Li, J. Lin, J. Ma, L. Song, H. Lin, B. Tang, et al., Methotrexate-camptothecin prodrug nanoassemblies as a versatile nanoplatform for biomodal imaging-guided self-active targeted and synergistic chemotherapy, ACS Appl. Mater. Interfaces 9 (40) (2017) 34650–34665.
[24] Y. Koda, K. Kuribayashi, H. Doi, K. Kitajima, Y. Nakajima, H. Ishigaki, et al., Irinotecan and gemcitabine as second-line treatment in patients with malignant pleural mesothelioma following platinum plus pemetrexed chemotherapy: a retrospective study, Oncology 99 (3) (2021).
[25] P. Koźmiński, P.K. Halik, R. Chesori, E. Gniazdowska, Overview of dual-acting drug methotrexate in different neurological diseases, autoimmune pathologies and cancers, Int. J. Mol. Sci. 21 (10) (2020) 3483.
[26] V.R. Barton, A. Toussi, S. Awasthi, M. Kiuru, Treatment of pediatric alopecia areata: A systematic review, J. Am. Acad. Dermatol. 86 (6) (2022) 1318–1334.
[27] A. Firooz, N. Bouzari, F. Mojtahed, H. Pazoki-Toroudi, M. Nassiri-Kashani, M. Davoudi, et al., Topical immunotherapy with diphencyprone in the treatment of extensive and/or long-lasting alopecia areata, J. Eur. Acad. Dermatol. 19 (3) (2005) 393–394.
[28] A. Spada, J. Emami, J.A. Tuszynski, A. Lavasanifar, The uniqueness of albumin as a carrier in nanodrug delivery, Mol. Pharm. 18 (5) (2021) 1862–1894.
[29] A.O. Elzoghby, W.M. Samy, N.A. Elgindy, Albumin-based nanoparticles as potential controlled release drug delivery systems, J. Control. Release 157 (2) (2012) 168–182.
[30] A. Loureiro, G. Azoia N, C. Gomes A, A. Cavaco-Paulo, Albumin-based nanodevices as drug carriers. Curr. Pharm. Des. 2016, 22(10):1371-90.
[31] F.-F. An, X.-H. Zhang, Strategies for preparing albumin-based nanoparticles for multifunctional bioimaging and drug delivery, Theranostics. 7 (15) (2017) 3667.
[32] S.-B. He, R.-T. Chen, Y.-Y. Wu, G.-W. Wu, H.-P. Peng, A.-L. Liu, et al., Improved enzymatic assay for hydrogen peroxide and glucose by exploiting the enzyme-mimicking properties of BSA-coated platinum nanoparticles, Microchim. Acta 186 (12) (2019) 778.
[33] Y. Nie, L. Li, Z. Wei, Recent advancements in Pt and Pt-free catalysts for oxygen reduction reaction, Chem. Soc. Rev. 44 (8) (2015) 2168–2201.
[34] S. Yu, Y. Cui, X. Guo, S. Chen, H. Sun, L. Wang, et al., Biocompatible bovine serum albumin stabilized platinum nanoparticles for the oxidation of morin, New J. Chem. 43 (22) (2019) 8774–8780.
[35] S.-B. He, R.-T. Chen, Y.-Y. Wu, G.-W. Wu, H.-P. Peng, A.-L. Liu, et al., Improved enzymatic assay for hydrogen peroxide and glucose by exploiting the enzyme-mimicking properties of BSA-coated platinum nanoparticles, Microchim. Acta 186 (12) (2019) 1–9.
[36] H. Nosrati, E. Attari, F. Abhari, M. Barsbay, M. Ghaffarlou, N. Mousazadeh, et al., Complete ablation of tumors using synchronous chemoradiation with bimetallic theranostic nanoparticles, Bioact. Mater. 7 (2022) 74–84.
[37] M.A. Thakar, S.S. Jha, K. Phasinam, R. Manne, Y. Qureshi, V.H. Babu, X ray diffraction (XRD) analysis and evaluation of antioxidant activity of copper oxide nanoparticles synthesized from leaf extract of Cissus vitiginea, Mater. Today:. Proc. 51 (2022) 319–324.

[38] C.A. Rodríguez-Proenza, J.P. Palomares-Báez, M.A. Chávez-Rojo, A.F. García-Ruiz, C.L. Azanza-Ricardo, A. Santoveña-Uribe, et al., Atomic surface segregation and structural characterization of PdPt bimetallic nanoparticles, Materials. 11 (10) (2018) 1882.
[39] H. Schwegmann, A.J. Feitz, F.H. Frimmel, Influence of the zeta potential on the sorption and toxicity of iron oxide nanoparticles on S. cerevisiae and E. coli, J. Colloid Interface Sci. 347 (1) (2010) 43–48.
[40] M. Alshamrani, Broad-Spectrum Theranostics and Biomedical Application of Functionalized Nanomaterials, Polymers 14 (6) (2022) 1221.
[41] L. Tang, X. Yang, Q. Yin, K. Cai, H. Wang, I. Chaudhury, et al., Investigating the optimal size of anticancer nanomedicine, Proc. Natl. Acad. Sci. 111 (43) (2014) 15344–15349.
[42] S. Honary, F. Zahir, Effect of zeta potential on the properties of nano-drug delivery systems-a review (Part 2), Trop. J. Pharm. Res. 12 (2) (2013) 265–273.
[43] F. Luo, Y. Li, M. Jia, F. Cui, H. Wu, F. Yu, et al., Validation of a Janus role of methotrexate-based PEGylated chitosan nanoparticles in vitro, Nanoscale Res. Lett. 9 (1) (2014) 1–13.
[44] N. Kohler, C. Sun, J. Wang, M. Zhang, Methotrexate-modified superparamagnetic nanoparticles and their intracellular uptake into human cancer cells, Langmuir 21 (19) (2005) 8858–8864.
[45] N. Kohler, C. Sun, A. Fichtenholtz, J. Gunn, C. Fang, M. Zhang, Methotrexate-immobilized poly (ethylene glycol) magnetic nanoparticles for MR imaging and drug delivery, Small 2 (6) (2006) 785–792.
[46] L. Wehl, C. von Schirnding, M.C. Bayer, O. Zhuzhgova, H. Engelke, T. Bein, Mesoporous Biodegradable Magnesium Phosphate-Citrate Nanocarriers Amplify Methotrexate Anticancer Activity in HeLa Cells, Bioconjug. Chem. 33 (4) (2022) 566–575.
[47] M. Petrovic, S. Popovic, D. Baskic, M. Todorovic, P. Djurdjevic, A. Ristic-Fira, et al., The effects of newly synthesized platinum (IV) complexes on cytotoxicity and radiosensitization of human tumour cells in vitro, Anticancer Res. 40 (9) (2020) 5001–5013.